Optical properties of human cranial bone in the spectral range from 800 to 2000 nm

Alexey N. Bashkatov*, Elina A. Genina, Vyacheslav I. Kochubey, Valery V. Tuchin
Saratov State University, 83, Astrakhanskaya str., Saratov, 410012, Russia

ABSTRACT

The optical properties of human cranial bones were measured in the wavelength range 800-2000 nm. The measurements were carried out using the commercially available spectrophotometer with an integrating sphere. The inverse adding-doubling method was used to determine the absorption and reduced scattering coefficients from the measurements.

Keywords: optical properties, absorption, scattering, bone, spectroscopy, infrared, in vitro

1. INTRODUCTION

Recent technological advancements in the photonics industry have real progress toward the development of non-invasive clinical functional cerebral imaging systems. Development of the optical methods in modern medicine in the areas of diagnostics and therapy has stimulated the investigation of optical properties of brain tissues, since the efficacy of optical probing of the tissues depends on the photon propagation and fluence rate distribution within irradiated tissues. Examples of diagnostic use are the monitoring of blood oxygenation and tissue metabolism[1,2], detection of brain malignancies[3], and recently suggested various techniques for optical imaging[4-6]. Therapeutic uses include applications in laser surgery[7] and in photodynamic therapy[3]. For these applications, the knowledge of tissue optical properties is of great importance for interpretation and quantification of diagnostic data, and to predict light distribution and absorbed dose for therapeutic use. Numerous investigations related to determination of tissue optical properties are available however the optical properties of many tissues have not been studied in a wide wavelength range.

Both development of new and optimization of already existing cerebral imaging systems require knowledge of optical properties of human cranial tissues, such as white and gray brain matter, dura mater, and scalp, in a wide wavelength range. Recently the optical properties of white and gray brain matter tissues have been measured by Yaroslavsky *et al*[8]. Genina *et al*[9] investigated the optical properties of human dura mater. The optical properties of skin in a wide wavelength range have been measured by Bashkatov *et al*[10]. The bone optical properties have been studied by several authors earlier in the visible and near infrared spectral ranges[11-15]. Firbank *et al*[11] and Ugryumova *et al*[15] have investigated the optical properties of bone tissues with integrating sphere technique. Firbank *et al*[11] have measured the optical properties in the spectral range 650-950 nm and Ugryumova *et al*[15] have measured the optical properties in the spectral range 520-960 nm. Tauber *et al*[13] have obtained bone optical properties on the five wavelengths (593, 635, 690, 780, and 830 nm) using computerized CCD camera image analysis. Bevilacqua *et al*[12] have measured the bone optical properties by spatially resolved diffuse reflectance (NIRS) and frequency domain photon migration (FDPM) techniques on the four wavelengths (674, 811, 849, and 956 nm). Pifferi *et al*[14] in the spectral range from 650 to 1000 nm measure the bone optical properties with time-resolved transmittance spectroscopy. However, in the infrared spectral range the optical properties of cranial bone have not been studied yet.

The goal of this paper is to measure the absorption and reduced scattering coefficients of human cranial bones in the wavelength range from 800 to 2000 nm.

2. MATERIALS AND METHODS

The measurements were carried out *in vitro* with ten bone samples, which obtained from *post-mortem* examinations of ten corps (seven men and three women). Age of the corps was between 16 and 70 years. The samples were obtained

* bash@optics.sgu.ru

Saratov Fall Meeting 2005: Optical Technologies in Biophysics and Medicine VII,
edited by Valery V. Tuchin, Proc. of SPIE Vol. 6163, 616310, (2006)
1605-7422/06/$15 · doi: 10.1117/12.697305

from parietal, temporal and temporoparietal bones of skull. Table 1 shows specification of the bone samples. All the samples are cortical (or compact) bones. Porosity of the bones is 5-10%[14]. The structural components of the bones consist of an inorganic matrix (largely mineralized) and an organic matrix[16,17]. The inorganic matrix contains calcium hydroxyapatite, which is responsible for the compressive strength of bone, and osteocalcium phosphate. The main components of the organic matrix are collagen, proteins, blood cells, and lipids[14]. Amount of the hydroapatite is 58%, the collagen content is 25%, water content is 12%, and carbohydrate content is 5%[18]. At the same time, Pifferi *et al*[14] have reported that the amount of bone mineral matrix is 16%, the lipid content is 54%, the proteins content is 16%, and water contributes 16%. It is the calcium and phosphorus component of the inorganic matrix that makes bone hard and rigid, and the arrangement of the collagen fibers in the organic matrix that makes it strong. In both men and women, bone mineral loss from the skeleton starts generally at ages 40 to 50. In women bone loss can be rapid immediately after menopause.

Table 1. Specification of the bone samples

N	Gender	Age, years	Autopsy location	Thickness, mm
1	Male	62	Right temporal bone	3.0±0.12
2	Female	38	Right temporal bone	5.0±0.49
3	Male	67	Right parietal bone	4.0±0.25
4	Male	44	Right parietal bone	3.0±0.17
5	Male	70	Right temporal bone	4.0±0.28
6	Male	37	Right temporoparietal bone	5.0±0.13
7	Female	47	Right parietal bone	2.5±0.41
8	Male	65	Right parietal bone	3.0±0.15
9	Male	67	Right parietal bone	3.0±0.16
10	Female	16	Right parietal bone	2.0±0.13

At microstructural length scales, cortical bone is organised into 200-300 μm diameter secondary osteons[19], which are composed of large vascular channels (50-90 μm diameter) surrounded by circumferential lamellar rings (3-7 μm thick), with so-called "cement lines" at the outer boundary[20]. At the nanostructural level, the lamellae are composed of organic type-I mineralized collagen fibers (up to 15 μm in length, 50-70 nm in diameter, and formed by regular arrangement of subnanostructural collagen molecules) bound and impregnated with inorganic carbonated apatite nanocrystals (about 30 nm in length and width, 2-3 nm in thickness)[21,22].

All samples were kept in saline at temperature about 5°C until spectroscopic measurements. The bone samples were measured during 4-6 h after autopsy. All the samples have area about 25×25 mm^2. The thickness of each bone sample was measured with a micrometer in several points over the sample surface and averaged. Precision of the single measurement was ±50 μm. Thickness of the samples are varied from 2.0±0.1 to 5.0±0.5 mm.

The total transmittance and diffuse reflectance measurements were performed in the 800-2000 nm wavelength range using the commercially available CARY-2415 ("Varian", Australia) spectrophotometer with an integrating sphere. Inner diameter of the sphere is 100 mm, size of the entrance port is 20×20 mm and diameter of the exit port is 16 mm. As a light source, a halogen lamp with filtering of the radiation in the studied spectral range is used in the measurements. The diameter of incident light beam on the tissue sample is 3 mm. Scan rate is 2 nm/sec. The measurements were carried out at room temperature about 20°C.

For processing the experimental data and determination of the optical properties of tissue, the inverse adding-doubling (IAD) method developed by Prahl *et al*[23] has been used. The method is widely used in tissue optics for processing the experimental data of spectrophotometry with integrating spheres[10,24-28]. This method allows one to determine the absorption (μ_a) and the reduced scattering coefficients $(\mu_s' = \mu_s(1-g))$ of a tissue from the measured values of the total transmittance and the diffuse reflectance. Here μ_s is the scattering coefficient, and g is the anisotropy factor of scattering. In these calculations the anisotropy factor has been fixed as 0.9, since this value is typical for the tissue in the visible and NIR spectral ranges[11,29]. The main advantage of the IAD method in comparison with many other methods of solution of the radiative transfer equation is connected with its validation for the arbitrary ratio of the absorption and

scattering coefficients[23]. The property of the IAD method becomes essentially important in the case of determination of the optical properties of tissues within strong absorption bands, when the values of the absorption and scattering coefficients become comparable. Other methods, for example, diffusion approximation[30] or Kubelka-Munk method[31], for their applicability require a fulfillment of the condition $\mu_a/\mu_s \ll 1$. The inverse Monte Carlo technique[32] can also be used for arbitrary ratio of μ_a and μ_s, but requires very extensive calculations. The main limitation of IAD method is connected with the possible loss of scattering radiation through lateral sides of a sample at calculations[33]. Loss of light through the sides of the sample and sample holder may erroneously increase the calculated value of the absorption coefficient. These losses depend on the physical size and geometry of the sample, i.e., the losses existing in the case, when the sizes of a sample do not exceed significantly the diameter of the incident beam. The size of the exit and the entrance ports of the integrating sphere are also important for errorless measurements of the total transmittance and the diffuse reflectance[33]. The tissue sample should completely cover the port in the integrating sphere, and the distance from the edge of irradiating beam on the sample to the edge of the port should be much larger than the lateral light propagation distance, which is determined as $1/(\mu_a + \mu_s')$. If this is not satisfied, then light will be lost out from the sides of the sample and the loss will be attributed to absorption, and so the absorption coefficient will be overestimated. These requirements have been met in our experiments, since maximal size of the sphere port does not exceed 20 mm, while the minimal size of the bone samples is 20 mm. In addition, using the absorption and the reduced scattering coefficients of the bone tissue presented below, in the next section, we calculated the lateral light propagation distance. For the tissue the maximal lateral light propagation distance is equal to 0.65 mm for the wavelength 1290 nm. Taking into account the diameter of the incident beam (3 mm), minimal size of a tissue sample has to be larger than 4.5 mm that was satisfied for each tissue sample under study. It is seen, that the lateral light propagation distance is smaller than the distance from the edge of the irradiating beam on the sample to the sample port edge. Besides, Pickering *et al*[33] have reported that area of tissue sample has to be smaller than the area of the inner surface of the integrating sphere. This requirement has also been met in our experiments, since the area of the inner surface of integrating sphere used in the measurements was 314.16 cm^2, while the area of the bone samples does not exceed 7.0 cm^2. Figure 1 shows geometry and parameters of the measurements in the transmittance and reflectance modes, respectively.

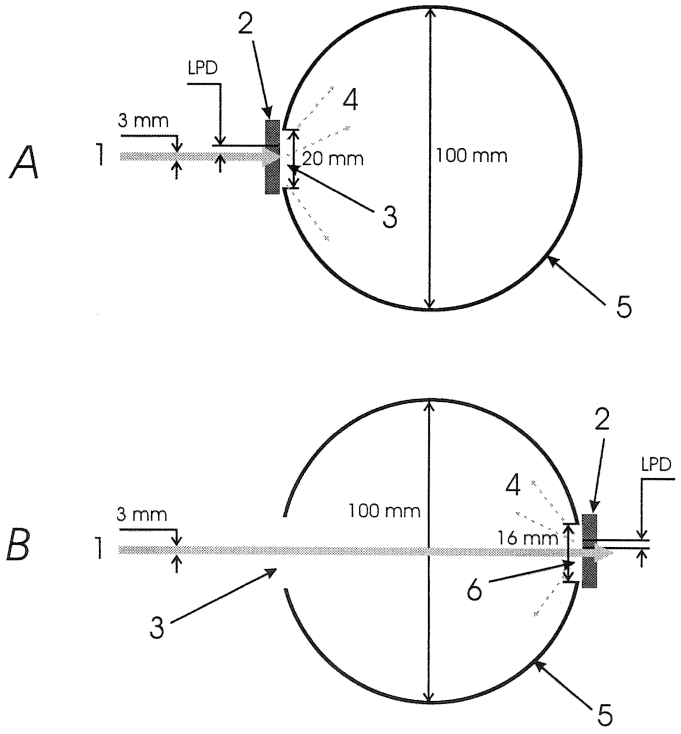

Figure 1: The geometry of the measurements in A) transmittance mode, B) reflectance mode. 1 - the incident beam (diameter 3 mm); 2 - the bone sample; 3 - the entrance port (square 20×20 mm); 4 - the transmitted (or diffuse reflected) radiation; 5 - the integrating sphere (inner diameter is 100 mm); 6 - the exit port (diameter 16 mm). LPD - the maximal value of lateral light propagation distance.

Calculation of tissue optical properties was performed for each wavelength point. The algorithm consists of the following steps: (a) the estimation of a set of optical properties; (b) the calculation of the reflectance and transmittance with the adding-doubling iterative method; (c) the comparison of the calculated with the measured values of the reflectance and the transmittance; (d) iteration of the above steps until a match (within the specified acceptance margin) is reached. With this iterative process the set of optical properties that yields the closest match to the measured values of reflectance and transmittance are taken as the optical properties of the tissue.

3. RESULTS AND DISCUSSION

Ten bone samples obtained from *post-mortem* examinations were used for the *in vitro* measurements. Figures 2-5 show the measured optical properties of the human cranial bone samples calculated by IAD method on the basis of measured values of the total transmittance and the diffuse reflectance. Figure 2 presents the wavelength dependence of the bone absorption coefficient. The vertical lines correspond to the values of standard deviation (*SD*), which is determined as: $SD = \sqrt{\sum_{i=1}^{n}\left(\overline{\mu}_a - \mu_{ai}\right)^2 \Big/ n(n-1)}$, where n = 10 is number of the measured tissue samples, μ_{ai} is the absorption coefficient of each sample, and $\overline{\mu}_a$ is the mean value of the absorption coefficient for each wavelength, which is calculated as $\sum_{i=1}^{n}\mu_{ai} \Big/ n$. In the spectral range, the absorption bands of water with maximums at 978, 1192, 1464 and 1930 nm are observed[34,35]. Absorption band with maximum at 1745 nm correspond to absorption band of lipids[36]. Increasing the standard deviation in the range of the absorption bands is connected with differences in the water content for different bone samples. Figure 3 and table 2 show the absorption coefficient values obtained in this paper (solid line) and presented by other authors (Firbank *et al*[11], Bevilacqua *et al*[12], Tauber *et al*[13], Pifferi *et al*[14], Ugryumova *et al*[15]) (symbols). Comparison of the data obtained in this study and presented by these authors shows an agreement between them in the spectral range 800-1000 nm. Insignificant differences between these data can be explained by differences in the used measuring techniques and the tissue samples preparation and storage methods.

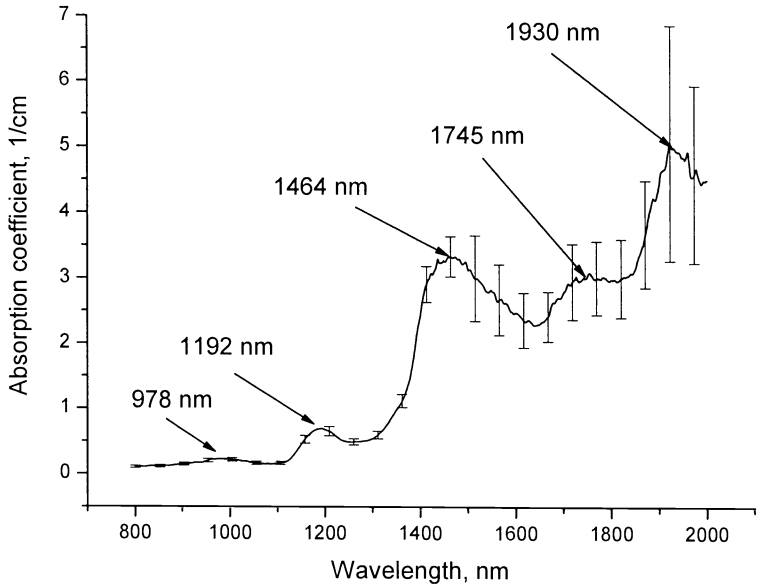

Figure 2: The wavelength dependence of the absorption coefficient of human cranial bone *in vitro*. The vertical lines show the standard deviation values.

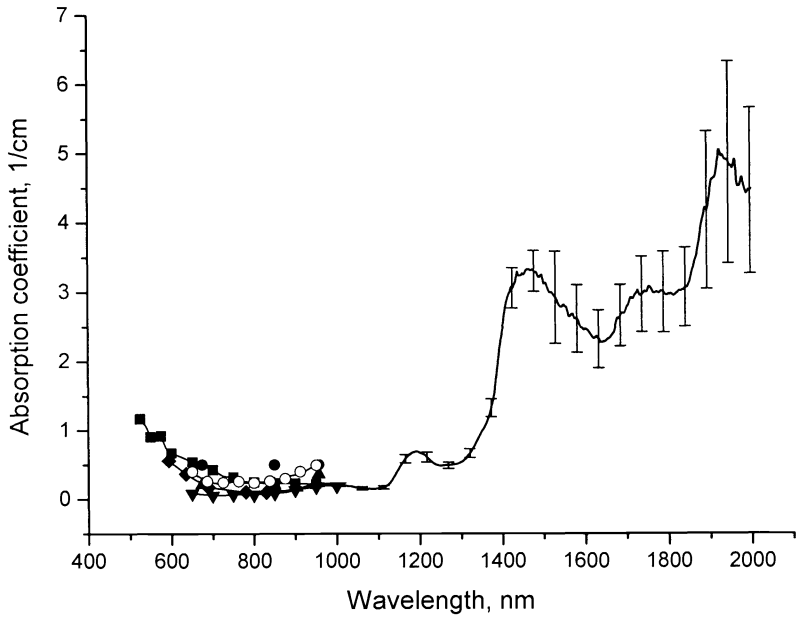

Figure 3: The wavelength dependence of the absorption coefficient of human cranial bone *in vitro*. The solid line corresponds to the averaged experimental data and the vertical lines show the standard deviation values. The symbols correspond to the experimental data presented in literature. The squares correspond to the data presented by Ugryumova *et al*[15], the circles and the up triangles correspond to the data of Bevilacqua *et al*[12] (NIR measurements and FDPM measurements, respectively). Down triangles correspond to the data of Pifferi *et al*[14], the diamonds correspond to the data of Tauber *et al*[13], and the open circles correspond to the data of Firbank *et al*[11].

Table 2. Comparison of bone absorption coefficients obtained in this work and presented in literature. In parenthesis shown standard deviation values.

λ, nm	this work	Pifferi *et al*[14]	Ugryumova *et al*[15]	Firbank *et al*[11]	Tauber *et al*[13]	Bevilacqua *et al*[12]	
						NIRS	FDPM
800	0.11(0.02)	0.07	0.25	0.24	-	-	-
830	0.11(0.02)	0.08	0.23	0.25	0.1(0.01)	-	-
850	0.11(0.02)	0.09	0.23	0.27	-	0.5(0.2)	0.22(0.01)
875	0.12(0.02)	0.11	0.23	0.3	-	-	-
900	0.15(0.02)	0.13	0.23	0.36	-	-	-
925	0.16(0.02)	0.19	0.23	0.41	-	-	-
956	0.21(0.03)	0.18	0.22	0.5	-	0.5(0.2)	0.36(0.01)
975	0.22(0.03)	0.21	-	-	-	-	-
1000	0.22(0.03)	0.19	-	-	-	-	-

Figures 4 and 5 present spectral dependence of the scattering properties (shown as reduced scattering coefficient) of the human bone samples. The dependence was obtained by averaging the scattering spectra measured for the ten samples. The vertical lines show standard deviation values of the reduced scattering coefficients of the bone tissue obtained during the measurements. Figure 4 shows that the reduced scattering coefficient decreases with wavelength increasing, which, in general, correspond to common nature of spectral behavior of the scattering characteristics of tissues[37-39]. However, in the spectral range from 1100 to 2000 nm the reduced scattering coefficient decreases non-monotonically with increasing of wavelength with peaks corresponding to the absorption bands in contrast to spectral behavior of bone scattering in the spectral range from 800 to 1100 nm, where the reduced scattering coefficient decreases smoothly with wavelength increasing.

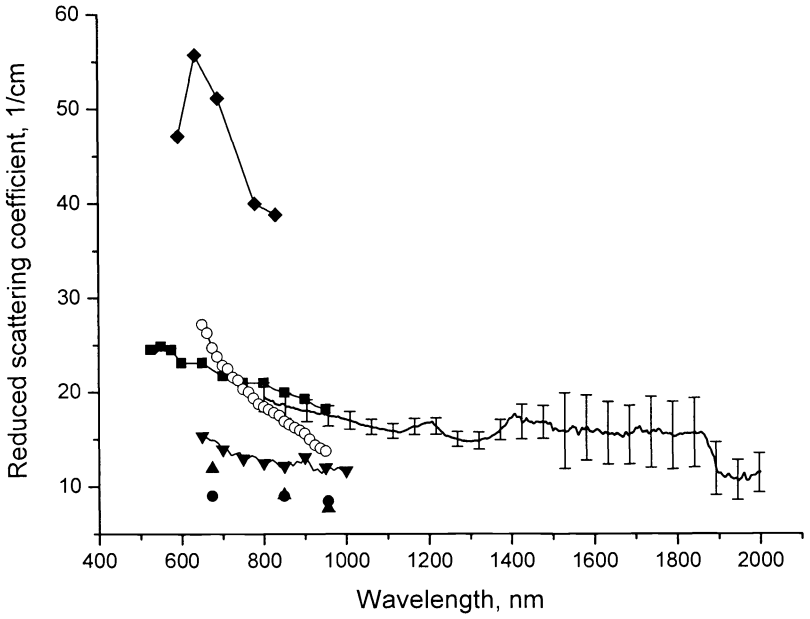

Figure 4: The spectral dependence of reduced scattering coefficient of human cranial bone *in vitro*. The solid line corresponds to the averaged experimental data and the vertical lines show the standard deviation values. The symbols correspond to the experimental data presented in literature. The squares correspond to the data presented by Ugryumova *et al*[15], the circles and the up triangles correspond to the data of Bevilacqua *et al*[12] (NIR measurements and FDPM measurements, respectively). Down triangles correspond to the data of Pifferi *et al*[14], the diamonds correspond to the data of Tauber *et al*[13], and the open circles correspond to the data of Firbank *et al*[11].

In contrast to the absorption properties, bone scattering properties, obtained by different authors with using different measuring methods, demonstrate very different magnitude and spectral behavior. A comparison of the data obtained by us (solid line) in the spectral range 800-950 nm with the data presented by Ugryumova *et al*[15] (squares) shows a good agreement between them. The data presented by Firbank *et al*[11] (open circles) also sufficiently close to data presented in this paper. In table 3 it is seen that discrepancy between these data not prevail 20%. However the reduced scattering coefficients presented by Firbank *et al*[11] significantly sharply decrease with wavelength increasing in comparison to data presented in this paper and obtained by other authors[12,14,15]. Besides Tauber *et al*[13] shows the reduced coefficient values significantly larger and Bevilacqua *et al*[12] and Pifferi *et al*[14] shows ones significantly smaller than presented in this paper. The discrepancies can be connected with natural dissipation of the tissue properties, differences in the used measuring techniques, methods of the tissue preparation and differences in bone types (cortical or trabecular) of the measured samples.

Tauber *et al*[13] measured bone optical properties obtained from temporal area of human skull using computerised CCD camera image analysis. As can be seen in figure 4 and table 3, the data obtained by Tauber *et al*[13] for skull bone significantly larger than presented in this paper and by Bevilacqua *et al*[12] and Firbank *et al*[11]. We assume that the differences can be connected with the measurement technique using by Tauber *et al*[13]. Ugryumova *et al*[15] and Firbank *et al*[11] in their investigations used the integrating spheres technique. In figure 4 and table 3 it is seen that data obtained by these authors are the more close to the data presented in this paper. Bevilacqua *et al*[12] and Pifferi *et al*[14] measured bones optical properties *in vivo* but Bevilacqua *et al*[12] measured the skull optical properties by spatially resolved diffuse reflectance and frequency domain photon migration techniques and Pifferi *et al*[14] measured the calcaneous bone optical properties with time-resolved transmittance spectroscopy. The differences between data presented by these authors and obtained by us are typical at comparison results of *in vivo* and *in vitro* measurements due to tissue dehydration before and during measurements. In this study, the investigated bone samples kept in saline and consequently the bones are not

dehydrated. We assume that possible reason of the differences is connected with replacing of bone interstitial fluid to saline. Since saline has refractive index smaller than interstitial fluid then this replacing increases the tissue scattering. Another reason of the differences between data presented by us and obtained by Pifferi *et al*[14] is connected with structure of investigated bones. In contrast to compact bone of skull investigated in this paper, Pifferi *et al*[14] investigated trabecular bone of calcaneous. The bone have component content similar to ones of compact bone but porosity of the trabecular bone are 50-90% [14] whereas compact bone has porosity 5-10%.

Table 3. Comparison of bone scattering properties obtained in this work and presented in literature. In parenthesis standard deviation values have shown.

λ, nm	this work	Pifferi *et al*[14]	Ugryumova *et al*[15]	Firbank *et al*[11]	Tauber *et al*[13]	Bevilacqua *et al*[12]	
						NIRS	FDPM
800	19.48(1.52)	12.5	21.0	18.4	-	-	-
830	18.71(1.48)	12.7	20.3	17.8	38.8(4.4)	-	-
850	18.73(1.37)	12.2	19.3	16.9	-	9.0(1)	9.1(0.23)
875	18.29(1.29)	12.4	19.6	16.3	-	-	-
900	18.03(1.19)	13.2	19.3	15.6	-	-	-
925	17.86(1.11)	11.8	18.6	14.4	-	-	-
956	17.51(1.07)	12.0	18.2	13.8	-	8.5(1)	7.7(0.19)
975	17.36(1.03)	11.9	-	-	-	-	-
1000	17.11(0.91)	11.7	-	-	-	-	-

In the spectral range 600-1500 nm for many tissues the reduced scattering coefficient decreases with the wavelength in accordance with a power law $\mu_s'(\lambda) = a\lambda^{-w}$ [37-39]. The wavelength exponent *w* characterizes the mean size of the tissue scatterers and defines spectral behavior of the reduced scattering coefficient. Figure 5 shows approximation of the wavelength dependence of the bone reduced scattering coefficient by the power law $\mu_s'(\lambda) = 1533.02\lambda^{-0.65}$, where λ is wavelength, nm. In the figure it is seen, that in the spectral range from 800 to 1100 nm this power law well approximates the experimental data, in contrast to the data in the spectral range from 1100 to 2000 nm.

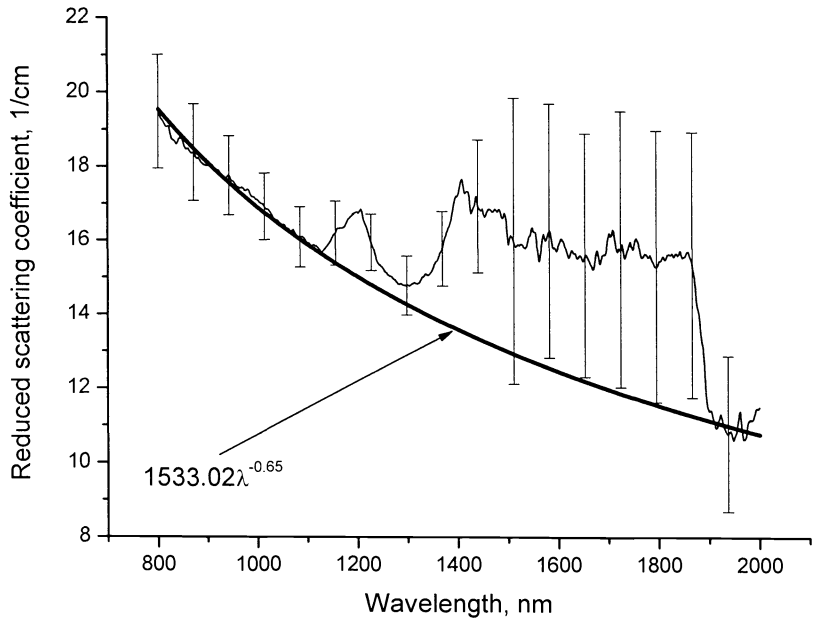

Figure 5: The spectral dependence of reduced scattering coefficient of human cranial bone *in vitro* and its approximation by power law. The symbols correspond to the averaged experimental data and the vertical lines show the standard deviation values.

Typically, the values of the wavelength exponent obtained for skin, eye sclera etc in the visible are in the range from 1 to 2, which is defined by the major scatterers type[29,38,39]. However, in the infrared the values of wavelength exponent are different. Approximating data of Troy and Thennadil[28] in the spectral range 1000-1250 nm and Du *et al*[40] in the spectral range 900-1350 nm we have obtained $w = 0.7$ and $w = 0.23$, respectively. Bashkatov *et al*[10] have obtained $w = 0.68$ for subcutaneous adipose tissue in the spectral range 600-2000 nm, and $w = 0.22$ for skin in this spectral range. Graaff *et al*[41] have predicted for the mixture of large spherical particles that $\mu_s' \sim \lambda^{-0.37}$. Thus, it is can be seen, that the wavelength exponent values obtained from different spectral ranges are various. One of the possible reasons for these large differences is the complex structure of the investigated tissues. For example, for skin, the scattering properties should be determined by the very thin collagen and elastin fibrils with size of 60-100 nm which are arranged in the bundles with size of 1-8 μm[42]. Diameter of effective scatterers for adipose tissue has been estimated as 0.8 μm[10]. The presence of the large so-called Mie scatterers produces a weak wavelength dependence of the scattering coefficient in the IR spectral range.

In this study, we have obtained for the bone tissue $w = 0.65 \pm 0.29$. The value is indicative of a slowly descending spectrum that is due to scatterers of large effective size, similar to what we have already found in the case of adipose tissue[10]. Pifferi *et al*[14] have reported the wavelength exponent value as 0.67 that is very close to the value obtained by us. Approximating data of Firbank *et al*[11], Bevilacqua *et al*[12], Tauber *et al*[13] and Ugryumova *et al*[15] we, respectively, found w equal to 1.68, 1.23 (NIRS measurement) and 0.14 (FDPM technique), 0.87 and 0.5. The obtained by us wavelength exponent value is close to the data of Pifferi *et al*[14], Tauber *et al*[13] and Ugryumova *et al*[15] but very different from data of Firbank *et al*[11] and Bevilacqua *et al*[12]. However averaging data of Bevilacqua *et al*[12] we have obtained $w = 0.69$ that also close to our data. For bone tissue a primary scatterers are mineralized collagen fibers (50-70 nm in diameter) and apatite nanocrystals (about 30 nm in length and width, and 2-3 nm in thickness). However, size of the scatterers is very small and though in the visible spectral range the Rayleigh scattering is dominant, but with the increase of the wavelength the contribution of the Rayleigh scattering is decreased sharply and in the IR the contribution is insignificant. In the infrared spectral range, apparently the vascular channels surrounded by circumferential lamellar rings composed by the mineralized collagen fibers and conglomerations of the apatite nanocrystals should determine the tissue scattering.

The effect of deviation of wavelength dependence of the reduced scattering coefficient from the power law dependence, i.e. the increase of the reduced scattering coefficients in the spectral range 1100-2000 nm with peaks corresponding to the absorption bands, can be connected with the increase of imaginary part of complex refractive index of the tissue scatterers in the range of the absorption bands. The increase of the imaginary part of the refractive index produces significant decrease of the anisotropy factor g, which together with the scattering coefficient μ_s of a tissue forms the tissue reduced scattering coefficient $\mu_s' = \mu_s(1-g)$. In the Refs. 40 and 43 it was experimentally shown that in the range of water absorption bands, with maximum at 1450 and 1930 nm, significant decrease of the anisotropy factor is observed that produces the increase of the reduced scattering coefficient and appearance of bands in its spectrum. Note that degree of the decrease of the anisotropy factor in the range of absorption bands is proportional to intensity of the absorption bands. The tissue scattering coefficient in the range of the absorption bands decreases only slightly[40,43]. This was confirmed by Fu and Sun[44] and Sun *et al*[45] who developed theory and computer model of light scattering on scattering particles immersed in an absorbing host medium. In the model these authors demonstrated that for large scatterers immersed in an absorbing medium decreasing of scattering coefficient and significant decreasing anisotropy factor (up to negative values) should be observed. In figure 2 one can see, that in the spectral range 800-1100 nm the absorption of the bone tissue is small. Hence, the scattering properties of the tissue are defined only by the real part of complex refractive index and the reduced scattering coefficient decreases rather monotonically with the wavelength (see figure 5). In the spectral range 1100-2000 nm the absorption bands of water and lipids are observed (see figure 2). The presence of the strong absorption bands leads to the fact that the scattering properties are formed not only under influence of the real, but also the imaginary part of a complex refractive index of the scattering centers, that produces increasing of the reduced scattering coefficient in the given spectral region with strong enough peaks in the range of the absorption bands. Insignificant shift of maxima of the peaks in spectrum of the reduced scattering coefficient in comparison with maxima of the absorption bands (see figures 2 and 5) can be explained by anomalous light dispersion, since within an absorption band the real part of refractive index corresponding to the short-wavelength wing of the absorption band goes down and at the long-wavelength wing it goes up.

4. CONCLUSION

The reduced scattering and the absorption coefficients of the human cranial bone *in vitro* have been determined over the wavelength range 800-2000 nm using the integrating sphere technique and the inverse adding-doubling method. In this spectral range the absorption bands of water and lipids with maxima at 978, 1192, 1464, 1745, and 1930 nm are observed. For the tissue in the spectral range from 800 to 1100 nm wavelength dependence of the reduced scattering coefficient can be described as $\mu_s'(\lambda) = 1533.02\lambda^{-0.65}$. The presented results can be used for the development and optimization of cerebral imaging systems and can be useful in tissue optics.

ACKNOWLEDGMENTS

The research described in this publication has been made possible, in part, by grant PG05-006-2 of U.S. Civilian Research and Development Foundation for the Independent States of the Former Soviet Union (CRDF) and the Russian Ministry of Science and Education, grants RUB1-570-SA-04 and BRHE Award Annex 07 Appendix 11 of CRDF, and grant of the Russian Federal Agency of Education Russian Federation 1.4.06. The authors thank N.A. Lakodina (Department of Optics and Biomedical Physics of Saratov State University) for the help in the experiments.

REFERENCES

1. D.A. Boas, M.A. Franceschini, A.K. Dunn, G. Strangman, "Noninvasive imaging of celebral activation with diffuse optical tomography," In: *In vivo optical imaging of brain function*, Ed. R.D. Frostig, CRC Press LLC, pp. 193-221, 2002.
2. E. Gratton, V. Toronov, U. Wolf, M. Wolf, A. Webb, "Measurement of brain activity by near-infrared light," *J. Biomed. Opt.*, **10**, 011008, 2005.
3. H. Kostron, A. Obwegeser, R. Jakober, "Photodynamic therapy in neurosurgery: a review," *J. Photochem. Photobiol. B*, **36**, 157-168, 1996.
4. P.J. Kirkpatrick, P. Smielewski, J.M.K. Lam, P. Al-Rawi, "Use of near infrared spectroscopy for the clinical monitoring of adult brain," *J. Biomed. Opt.*, **1**, 363-372, 1996.
5. S. Fantini, D. Hueber, M.A. Franceschini, E. Gratton, W. Rosenfeld, P.G. Stubblefield, D. Maulik, M.R. Stankovic, "Non-invasive optical monitoring of the newborn piglet brain using continuous-wave and frequency-domain spectroscopy," *Phys. Med. Biol.,* **44**, 1543-1563, 1999.
6. J.C. Hebden, A. Gibson, T. Austin, R.M. Yusof, N. Everdell, D.T. Delpy, S.R. Arridge, J.H. Meek, J.S. Wyatt, "Imaging changes in blood volume and oxygenation in the newborn infant brain using three-dimensional optical tomography," *Phys. Med. Biol.*, **49**, 1117-1130, 2004.
7. H. Bertalanffy, L. Benes, T. Miyazawa, O. Alberti, A.M. Siegel, U. Sure, "Cerebral cavernomas in the adult. Review of the literature and analysis of 72 surgically treated patients," *Neurosurgery Review*, **25**, 1-53, 2002.
8. A.N. Yaroslavsky, P.C. Schulze, I.V. Yaroslavsky, R. Schober, F. Ulrich, H.-J. Schwarzmaier, "Optical properties of selected native and coagulated human brain tissues *in vitro* in the visible and near infrared spectral range," *Phys. Med. Biol.*, **47**, 2059-2073, 2002.
9. E.A. Genina, A.N. Bashkatov, V.I. Kochubey, V.V. Tuchin, "Optical clearing of human dura mater," *Optics and Spectroscopy*, **98**, 470-476, 2005.
10. A.N. Bashkatov, E.A. Genina, V.I. Kochubey, V.V. Tuchin, "Optical properties of human skin, subcutaneous and mucous tissues in the wavelength range from 400 to 2000 nm," *J. Phys. D: Appl. Phys.*, **38**, 2543-2555, 2005.
11. M. Firbank, M. Hiraoka, M. Essenpreis, D.T. Delpy, "Measurement of the optical properties of the skull in the wavelength range 650-950 nm," *Phys. Med. Biol.*, **38**, 503-510, 1993.
12. F. Bevilacqua, D. Piguet, P. Marquet, J.D. Gross, B.J. Tromberg, C. Depeursinge, "*In vivo* local determination of tissue optical properties: applications to human brain," *Appl. Opt.*, **38**, 4939-4950, 1999.
13. S. Tauber, R. Baumgartner, K. Schorn, W. Beyer, "Lightdosimetric quantitative analysis of the human petrous bone: experimental study for laser irradiation of the cochlea," *Lasers Surg. Med.*, **28**, 18-26, 2001.
14. A. Pifferi, A. Torricelli, P. Taroni, A. Bassi, E. Chikoidze, E. Giambattistelli, R. Cubeddu, "Optical biopsy of bone tissue: a step toward the diagnosis of bone pathologies," *J. Biomed. Opt.*, **9**, 474-480, 2004.

15. N. Ugryumova, S.J. Matcher, D.P. Attenburrow, "Measurement of bone mineral density via light scattering," *Phys. Med. Biol.*, **49**, 469-483, 2004.
16. A. Boskey, R. Mendelsohn, "Infrared analysis of bone in health and disease," *J. Biomed. Opt.*, **10**, 131102, 2005.
17. J.W. Ager III, R.K. Nalla, K.L. Breeden, R.O. Ritchie, "Deep-ultraviolet Raman spectroscopy study of the effect of aging on human cortical bone," *J. Biomed. Opt.*, **10**, 034012, 2005.
18. D.R. White, E.M. Widdowson, H.Q. Woodard, W.T. Dickerson, "The composition of body tissues," *Br. J. Radiol.*, **64**, 149-159, 1991.
19. J.D. Currey, "'Osteons' in biomechanical literature," *J. Biomech.*, **15**, 717, 1982.
20. S. Weiner, H.D. Wagner, "The material bone: structure-mechanical function relations," *Annu. Rev. Mater. Sci.*, **28**, 271-298, 1998.
21. A.S. Posner, *Bone mineral and the mineralisation process. Bone and Mineral Research,* Ed. W.A. Peck, Amsterdam: Elsevier, pp. 65-116, 1987.
22. J.-Y. Rho, L. Kuhn-Spearing, P. Zioupos, "Mechanical properties and the hierarchical structure of bone," *Med. Eng. Phys.*, **20**, 92-102, 1998.
23. S.A. Prahl, M.J.C. van Gemert, A.J. Welch, "Determining the optical properties of turbid media by using the adding-doubling method," *Appl. Opt.*, **32**, 559-568, 1993.
24. B. Nemati, H.G. Rylander III, A.J. Welch, "Optical properties of conjunctiva, sclera, and the ciliary body and their consequences for transscleral cyclophotocoagulation," *Appl. Opt.*, **35**, 3321-3327, 1996.
25. J.F. Beek, P. Blokland, P. Posthumus, M. Aalders, J.W. Pickering, H.J.C.M. Sterenborg, M.J.C. van Gemert, "*In vitro* double-integrating-sphere optical properties of tissues between 630 and 1064 nm," *Phys. Med. Biol.*, **42**, 2255-2261, 1997.
26. A.N. Bashkatov, E.A. Genina, V.I. Kochubey, V.V. Tuchin, "Estimation of wavelength dependence of refractive index of collagen fibers of scleral tissue," *Proc.* SPIE, **4162**, 265-268, 2000.
27. D.K. Sardar, M.L. Mayo, R.D. Glickman, "Optical characterization of melanin," *J. Biomed. Opt.*, **6**, 404-411, 2001.
28. T.L. Troy, S.N. Thennadil, "Optical properties of human skin in the near infrared wavelength range of 1000 to 2200 nm," *J. Biomed. Opt.*, **6**, 167-176, 2001.
29. V.V. Tuchin, *Tissue Optics: Light Scattering Methods and Instruments for Medical Diagnosis* Vol. TT38 Washington: SPIE Press, 2000.
30. T.J. Farrell, M.S. Patterson, B.C. Wilson, "A diffusion theory model of spatially resolved, steady-state diffuse reflectance for the noninvasive determination of tissue optical properties in vivo," *Med. Phys.*, **19**, 879-888, 1992.
31. W.E. Vargas, "Inversion methods from Kubelka-Munk analysis," *J. Opt. A: Pure Appl. Opt.*, **4**, 452-456, 2002.
32. I.V. Yaroslavsky, A.N. Yaroslavsky, T. Goldbach, H.-J. Schwarzmaier, "Inverse hybrid technique for determining the optical properties of turbid media from integrating-sphere measurements," *Appl. Opt.*, **35**, 6797-6809, 1996.
33. J.W. Pickering, S.A. Prahl, N. van Wieringen, J.F. Beek, H.J.C.M. Sterenborg, M.J.C. van Gemert, "Double-integrating-sphere system for measuring the optical properties of tissue," *Appl. Opt.*, **32**, 399-410, 1993.
34. K.F. Palmer, D. Williams, "Optical properties of water in the near infrared," *J. Opt. Soc. Am.*, **64**, 1107-1110, 1974.
35. L. Kou, D. Labrie, P. Chylek, "Refractive indices of water and ice in the 0.65-2.5μm spectral range," *Appl. Opt.*, **32**, 3531-3540, 1993.
36. K.A. Martin, "Direct measurement of moisture in skin by NIR spectroscopy," *J. Soc. Cosmet. Chem.*, **44**, 249-261, 1993.
37. J.R. Mourant, T. Fuselier, J. Boyer, T.M. Johnson, I.J. Bigio, "Predictions and measurements of scattering and absorption over broad wavelength ranges in tissue phantoms," *Appl. Opt.*, **36**, 949-957, 1997.
38. J.M. Schmitt, G. Kumar, "Optical scattering properties of soft tissue: a discrete particle model," *Appl. Opt.*, **37**, 2788-2797, 1998.
39. R.K. Wang, "Modelling optical properties of soft tissue by fractal distribution of scatterers," *J. Modern Opt.*, **47**, 103-120, 2000.
40. Y. Du, X.H. Hu, M. Cariveau, G.W. Kalmus, J.Q. Lu, "Optical properties of porcine skin dermis between 900 nm and 1500 nm," *Phys. Med. Biol.*, **46**, 167-181, 2001.

41. R. Graaff, J.G. Aarnoudse, J.R. Zijp, P.M.A. Sloot, F.F.M. de Mul, J. Greve, M.H. Koelink, "Reduced light-scattering properties for mixtures of spherical particles: a simple approximation derived from Mie calculations," *Appl. Opt.*, **31**, 1370-1376, 1992.
42. I.S. Saidi, S.L. Jacques, F.K. Tittel, "Mie and Rayleigh modeling of visible-light scattering in neonatal skin," *Appl. Opt.*, **34**, 7410-7418, 1995.
43. J.-P. Ritz, A. Roggan, C. Isbert, G. Muller, H. Buhr, C.-T. Germer, "Optical properties of native and coagulated porcine liver tissue between 400 and 2400 nm," *Lasers Surg. Med.*, **29**, 205-212, 2001.
44. Q. Fu, W. Sun, "Mie theory for light scattering by a spherical particle in an absorbing medium," *Appl. Opt.*, **40**, 1354-1361, 2001.
45. W. Sun, N.G. Loeb, B. Lin, "Light scattering by an infinite circular cylinder immersed in an absorbing medium," *Appl. Opt.*, **44**, 2338-2342, 2005.